

## Supplementary Information

### Visible-light harvesting 2D copper-cluster-based MOFs as efficient ROS generators for selective oxidation of amines

Huilin Huang,<sup>a\*</sup> Qiong Yang,<sup>a</sup> Kun Yao,<sup>a</sup> Wenchao Geng<sup>a</sup> and Xu Jing<sup>b\*</sup>

<sup>a</sup>School of Chemical and Printing Dyeing Engineering, Henan University of Engineering, Zhengzhou, 451191, P. R. China

<sup>b</sup>State Key Laboratory of Fine Chemicals, School of Chemistry, Dalian University of Technology, Dalian 116024, P. R. China

Corresponding Authors

\* E-mail: huanghuilin321@126.com, xjing@dlut.edu.cn

#### Contents

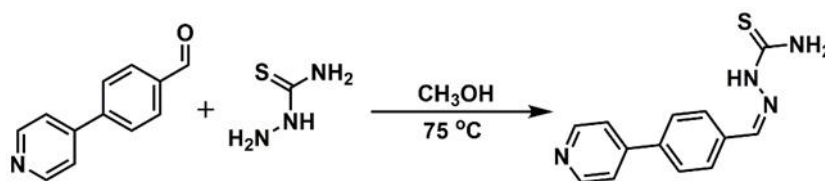
1. Experimental Section
2. Single Crystal X-ray Crystallography
3. Characterizations of Cu-BPYC
4. Catalysis Details
5. References

## 1. Experimental Section

### Materials and methods

All starting chemicals and reagents were commercially available and used without further purification unless specifically mentioned. BPYC was synthesized based on reported literature.<sup>51</sup> <sup>1</sup>H NMR data were collected on a Varian INOVA 400M spectrometer at ambient temperature. The powder XRD diffractograms were obtained on a Rigaku D/Max-2400 X-ray diffractometer with a sealed Cu tube ( $\lambda = 1.54178 \text{ \AA}$ ). Thermogravimetric analyses (TGA) were performed from 20 to 800 °C at a heating rate of 10 °C min<sup>-1</sup> and a N<sub>2</sub> flow rate of 50 mL min<sup>-1</sup>. Fourier transform infrared (FT-IR) spectra were collected in the range of 400-3500 cm<sup>-1</sup> as KBr pellets on Thermo Fisher-6700. The solid UV-vis spectra were recorded on a Hitachi U-4100 UV-vis-NIR spectrophotometer. X-ray photoelectron spectroscopy (XPS) was measured using Thermo ESCALAB-250XI. <sup>1</sup>H NMR spectra were recorded in the designated solvents on Varian DLG 400 M spectrometer with chemical shift in ppm. The solid fluorescent spectrum was measured on an Edinburgh FIS1000 instrument. The time-resolved luminescence spectrum was measured on an Edinburgh FLS1000 spectrometer. Electron paramagnetic resonance (EPR) experiments were measured on Bruker E500 instrument. The light sources was 450 nm LED, which were purchased from the Beijing China Education Au-light Co., Ltd.

### The synthetic routes of the BPYC



BPYC was synthesized as literature reported.<sup>51</sup> 4-(Pyridin-4-yl)benzaldehyde (1.8 g, 0.010 mol) and thiosemicarbazide (0.92 g, 0.0101 mol) were dissolved in dry methanol (40 mL). The resulting solution was heated and stirred at 75 °C for 8 hours. Upon completion of the reaction, the light yellow solid that formed was separated by suction filtration and washed with a small amount of cold, dry methanol to remove impurities. The solid product was then dried under vacuum to constant weight. The final target

compound obtained was 2.3 g, yielding 91%. (<sup>1</sup>H NMR (400 MHz, DMSO-*d*<sub>6</sub>) δ 11.56 (s, 1H), 8.66 (dd, *J* = 4.6, 1.5 Hz, 2H), 8.30 (s, 1H), 7.97 (d, *J* = 8.4 Hz, 2H), 7.86 (d, *J* = 8.4 Hz, 2H), 7.77 (dd, *J* = 4.6, 1.6 Hz, 2H); <sup>13</sup>C NMR (101 MHz, DMSO-*d*<sub>6</sub>) δ = 178.57, 150.74, 146.64, 141.88, 138.53, 135.56, 128.51, 127.51, 121.56.)

### **Preparation of Cu-BPYC**

At room temperature, 3 mL of a 0.03 mM copper(I) iodide (CuI) solution in acetonitrile (CH<sub>3</sub>CN) was slowly diffused into 3.0 mL of a 0.015 mM BPYC ligand solution in N,N'-dimethylformamide (DMF), with a buffer solvent of 12 mL DMF/CH<sub>3</sub>CN mixture (v/v = 1 : 8). After two weeks, yellow block crystals appeared in the glass tube. Crystals appropriate for X-ray structural analysis were obtained after filtration. Supercritical carbon dioxide was used for additional drying of crystals. Yield: 75% (based on ligands BPYC).

### **TMB Oxidation Measurement**

First, 1.5 mL of water and 1.5 mL of 0.2 M HAC/NaAc buffer solution were measured, and then 1.5 mg of TMB was added to prepare the mixed solution. Under blue LED irradiation, 200.0 μL of 1 mg/mL Cu-BPYC suspension was added to the mixed solution. Samples were collected at various intervals for UV-Vis analyses.

### **EPR detection of super oxygen radical**

The ROS generated by Cu-BPYC have been detected by EPR in the presence of DMPO and TEMP, respectively. Typically, 20.0 μL DMPO or TEMP in 1 mL CH<sub>3</sub>CN was mixed with 0.5 mL of Cu-BPYC/CH<sub>3</sub>CN suspension (0.5 mg/mL). The formed mixture (200 μL) was added into the EPR tube.

### **Photoelectrochemical Measurements**

Through CHI 760E electrochemical workstation, photocurrent was measured in a standard three-electrode system with the photocatalyst-coated FTO as the working electrode, Pt plate as the counter electrode and Ag/AgCl as the reference electrode. A 450 nm LED was used as light source. A 1.0 M KCl solution was used as electrolyte. The catalyst (2.0 mg) was added into a mixed solution with 20.0 μL of 5 wt % Nafion and 1 mL of ethanol, and the working electrodes were prepared by dropping the suspension

(100  $\mu\text{L}$ ) onto the surface of a FTO plate with an area of 1.0  $\text{cm}^2$ . EIS was performed with a 20.0  $\mu\text{L}$  suspension on the working electrode, the measurements were carried out with KCl (1.0 M) as the supporting electrolyte, Ag/AgCl electrode as a reference electrode and Pt wire as counter electrode.

## 2. Single Crystal X-ray Crystallography

The intensity data were collected on a Bruker SMART APEX CCD diffractometer equipped with a graphite-monochromated Mo K $\alpha$  radiation source (wavelength  $\lambda = 0.71073 \text{ \AA}$ ). The data collection was controlled using the SMART software, and data reduction was performed with the SAINT program.<sup>S2-S3</sup> The crystal structure was solved by direct methods, and subsequent refinement of the structural model was carried out using the SHELXL-2014 program based on full-matrix least-squares techniques.<sup>S4</sup> In the structural refinement of Cu-BPYC, all of the non-hydrogen atoms were refined anisotropically. The hydrogen atoms within the ligand backbones were fixed geometrically at calculated distances and allowed to ride on the parent non-hydrogen atoms. The SQUEEZE subroutine in PLATON was used.<sup>S5</sup>

**Table S1.** Crystal data and structure refinements.

Compound	Cu-BPYC
Empirical formula	C <sub>13</sub> H <sub>12</sub> Cu <sub>2</sub> I <sub>2</sub> N <sub>4</sub> S
Formula weight	637.21
Temperature/K	200
Crystal system	Triclinic
Space group	P-1
a/Å	9.2042(7)
b/Å	9.2118(7)
c/Å	12.3630(9)
α/°	99.783(2)
β/°	99.2390(10)
γ/°	119.037(2)
Volume/Å <sup>3</sup>	866.47(11)
Z	2
ρ <sub>calc</sub> /g·cm <sup>-3</sup>	2.442
μ/mm <sup>-1</sup>	6.137
F(000)	596.0
Crystal size/mm <sup>3</sup>	0.12 × 0.11 × 0.10
Radiation	MoKα (λ = 0.71073)
2 theta range for data collection/°	5.134 to 61.09
Index ranges	-13 ≤ h ≤ 11, -9 ≤ k ≤ 13, -16 ≤ l ≤ 17
Reflections collected	8815
Independent reflections	5290 [R <sub>int</sub> = 0.0184, R <sub>sigma</sub> = 0.0368]
Data/restraints/parameters	5290/0/200
Goodness-of-fit on F <sup>2</sup>	1.021
Final R indexes [I ≥ 2σ (I)]	R1 = 0.0307, wR2 = 0.0612
Final R indexes [all data]	R1 = 0.0420, wR2 = 0.0648
Largest diff. peak/hole / e Å <sup>-3</sup>	1.19/-0.95
CCDC number	2385286

### 3. Characterizations of Cu-BPYC

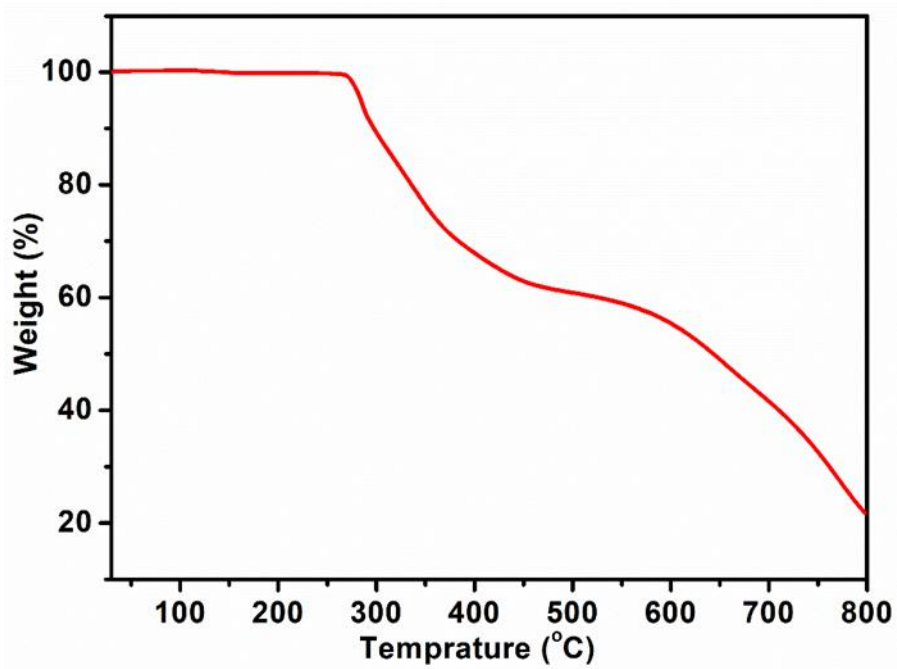


**Figure S1.** TGA figure of the prepare Cu-BPYC with heating rates of 10 °C/min, exhibiting a stable platform from 25 °C to 270 °C.

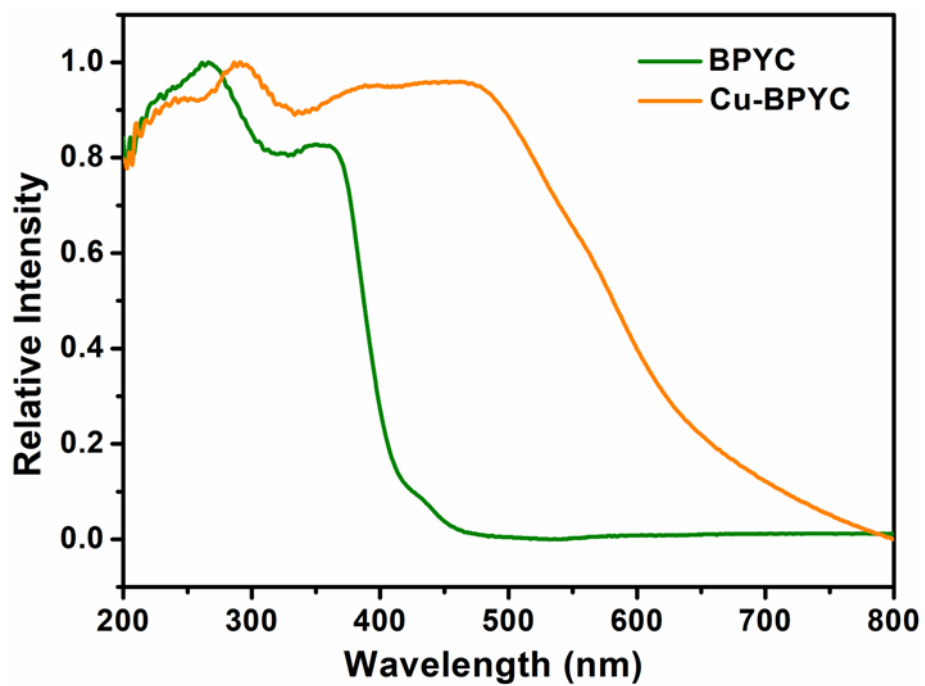
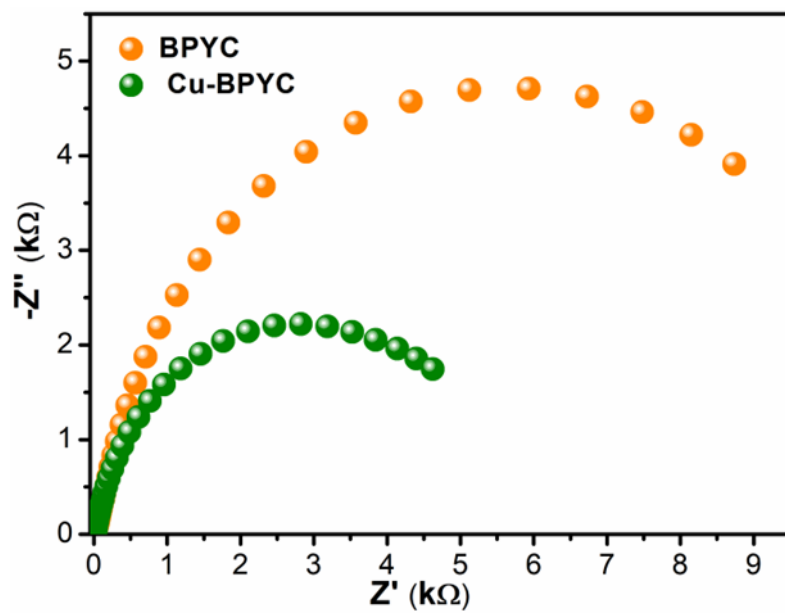
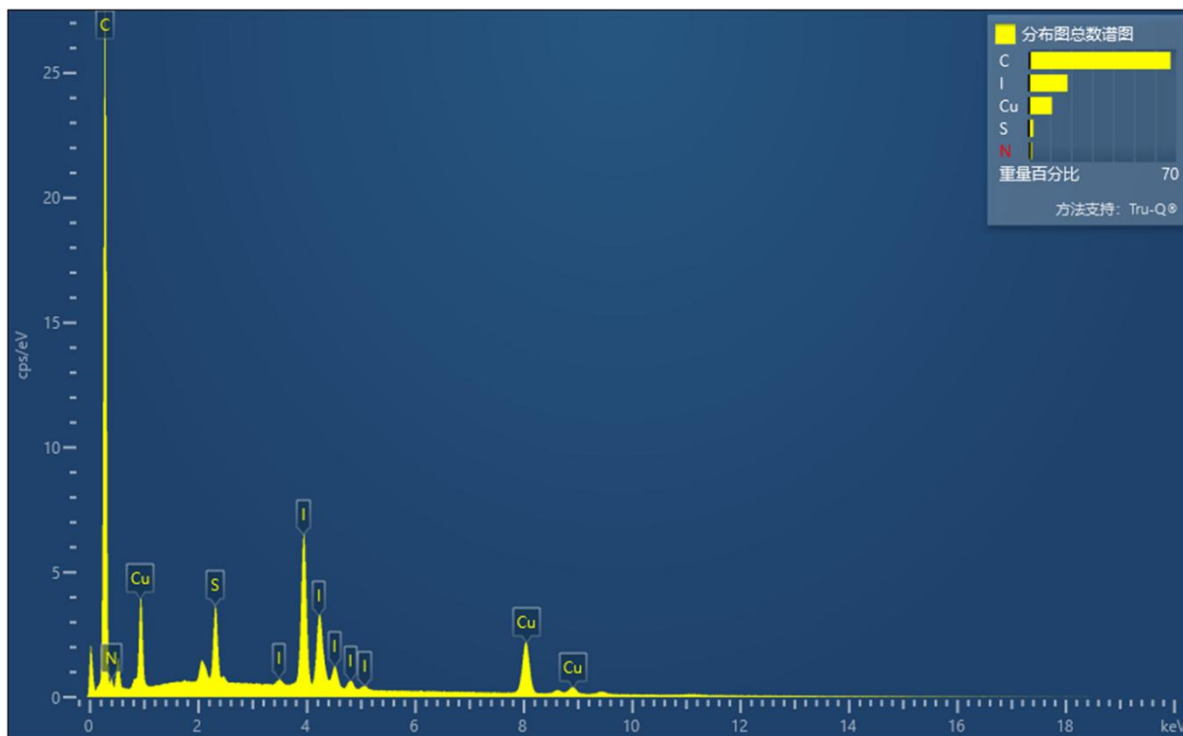


Figure S2. Solid UV-vis spectra of Cu-BPYC and the free ligand.





**Figure S3.** EIS plots (b) of Cu-BPYC, and BPYC under the same conditions.



**Figure S4.** The EDS spectra of Cu-BPYC.

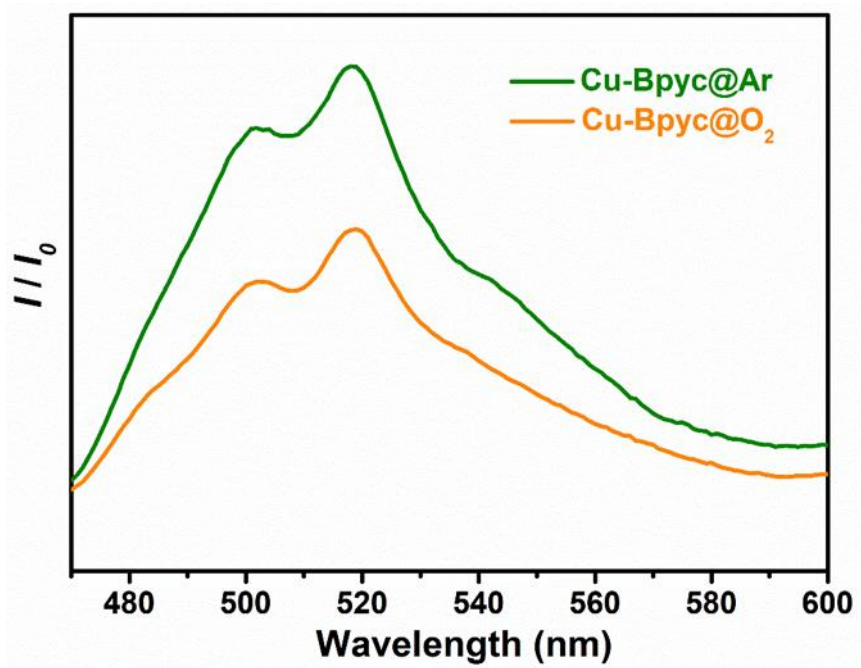


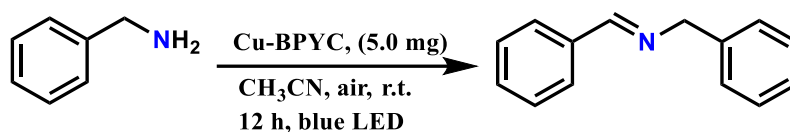
**Figure S5.** Luminescence decays of Cu-BPyc suspensions with (orange) or without (green) O<sub>2</sub>.

## 4. Catalysis Details

### 4.1 General Procedure Photocatalytic Oxidation of Amine Coupling

Typically, 4.0 mg of Cu-BPYC, 5 mL of acetonitrile, a 1 cm stir bar, and the substrate were sequentially added to a 15.0 mL quartz reaction tube. The reaction was carried out under a 450 nm LED lamp, at room temperature, in an air atmosphere, and lasted for 10 hours.

**Table S2. Visible-Light-Driven Photocatalytic Oxidative Coupling of Benzylamine<sup>a</sup>**



Entry	Variation from the standard conditions	Yield (%) <sup>b</sup>
1 <sup>a</sup>	None	91
2	No Cu-BPYC	trace
3	No light	trace
4	Ar instead of Air	trace
5	CuI instead of Cu-BPYC	32
6	BPYC instead of Cu-BPYC	trace
7	Cyclohexane instead of Cu-BPYC	8
8	green LED instead of blue LED	52
9	red LED instead of blue LED	6
10	2 equiv. DABCO	32
11	2 equiv. BQ	75
12	Phenylmethanamine instead of Benzylamine	trace

[a] Reaction conditions: photocatalyst (4 mg), benzylamine (0.2 mmol) and solvent (2.0 mL) under air for 10 h; The yields were determined by <sup>1</sup>H NMR with 1,3,5-Trimethoxybenzene as the internal standard.

## 4.2 Photocatalytic H<sub>2</sub>O<sub>2</sub> production

The production of H<sub>2</sub>O<sub>2</sub> was analyzed by the well-established iodimetry method.<sup>S39</sup> Typically, 50 μL 0.4 mol·L<sup>-1</sup> potassium iodide and 50 μL 0.1 mol L<sup>-1</sup> potassium hydrogen phthalate solutions were mixed followed by the addition of 2.0 mL of the reaction supernatant by centrifugation, which was kept over 30 min to ensure that H<sub>2</sub>O<sub>2</sub> sufficiently reacted with I<sup>-</sup> under acidic conditions to form I<sup>3-</sup>. Then the mixed solution was diluted 50 times and measured by UV-Vis spectroscopy. The total amount of H<sub>2</sub>O<sub>2</sub> generated was estimated according to the standard curve of the absorbance at 350 nm of I<sup>3-</sup> ( $H_2O_2 + 3I^- + 2H^+ \rightarrow I_3^- + 2H_2O$ ).

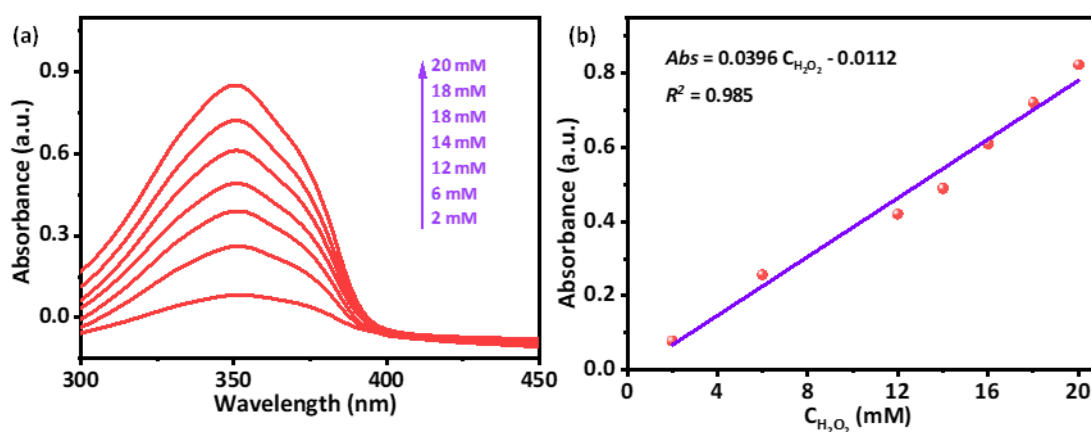


**Figure S6.** (a) UV-Vis absorption spectra of different H<sub>2</sub>O<sub>2</sub> concentrations by iodimetry. (b) The standard linear relationship between the absorption and H<sub>2</sub>O<sub>2</sub> concentrations.

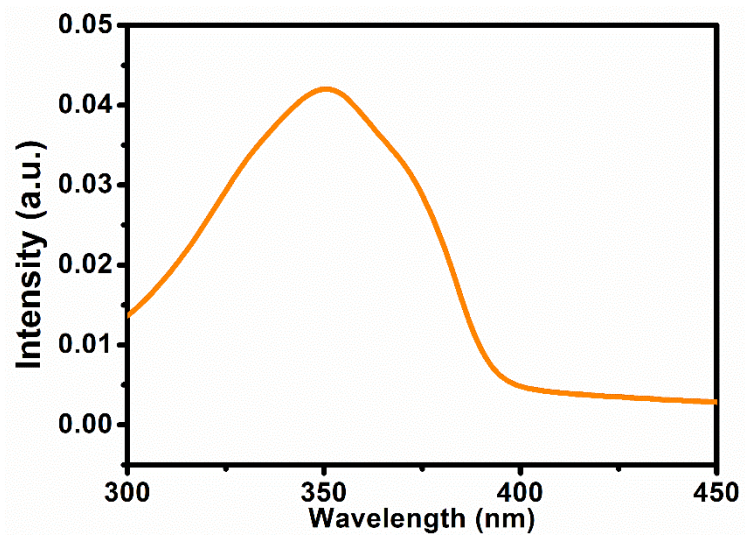


**Figure S7.** UV-Vis absorption spectrum of  $\text{H}_2\text{O}_2$  generation in the reaction solution after 4 hours of Cu-BPYC photocatalytic oxidation of benzylamine.

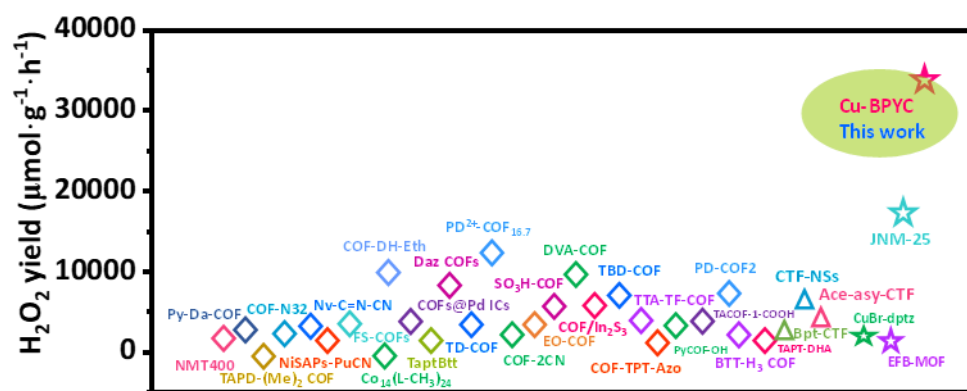


**Figure S8.** Summary of photocatalytic H<sub>2</sub>O<sub>2</sub> production rates of Cu-BPYC and other recently reported photocatalysts.

**Table S3.** Comparison of photocatalytic H<sub>2</sub>O<sub>2</sub> production rates of Cu-BPYC and other recently reported photocatalysts.<sup>S6-S38</sup>

Catalysts	Reaction pathway	H <sub>2</sub> O <sub>2</sub> yield (μmol·g <sup>-1</sup> ·h <sup>-1</sup> )	Reference
<b>Cu-BPYC</b>	Benzylamine oxidation, ORR	33575	<b>This work</b>
NMT400	ORR	1695.3	S6
Py-Da-COF	ORR, OER	1242	S7
TAPD-(Me) <sub>2</sub> COF	ORR	234.52	S8
COF-N32	ORR	605	S9
Nv-C=N-CN	ORR	3093	S10
NiSAPs-PuCN	ORR	342.2	S11
FS-COFs	ORR	3904.2	S12
Co <sub>14</sub> (L-CH <sub>3</sub> ) <sub>24</sub>	ORR, WOR	146.6	S13
COF-DH-Eth	ORR	9212	S14
TAPTTFPA COFs@Pd ICs	ORR	2143	S15
TaptBtt	ORR, WOR	1407	S16
Daz COFs	ORR	7327	S17
TD-COF	ORR, WOR	4060	S18
PD <sup>2+</sup> -COF <sub>16.7</sub>	ORR	11965	S19
COF-2CN	ORR	1601	S20
EO-COF	ORR	2675	S21
SO <sub>3</sub> H-COF	ORR	4971	S22
DVA-COF	ORR	8450	S23
COF/In <sub>2</sub> S <sub>3</sub>	ORR	5713.2	S24



TBD-COF	ORR, WOR	6085	S25
TTA-TF-COF	ORR, WOR	3343	S26
COF-TPT-Azo	ORR	1498	S27
PyCOF-OH	ORR, WOR	2961	S28
TACOF-1-COOH	ORR	3542	S29
PD-COF2	ORR	6103	S30
BTT-H3 COF	ORR	1588	S31
TAPT-DHA	ORR	1629	S32
Bpt-CTF	ORR	3268.1	S33
CTF-NSs	ORR, WOR	5007	S34
Ace-asy-CTF	ORR	2594	S35
CuBr-dptz	ORR	1874	S36
EFB-MOF	ORR	1676	S37
JNM-25	ORR, OER	17476	S38

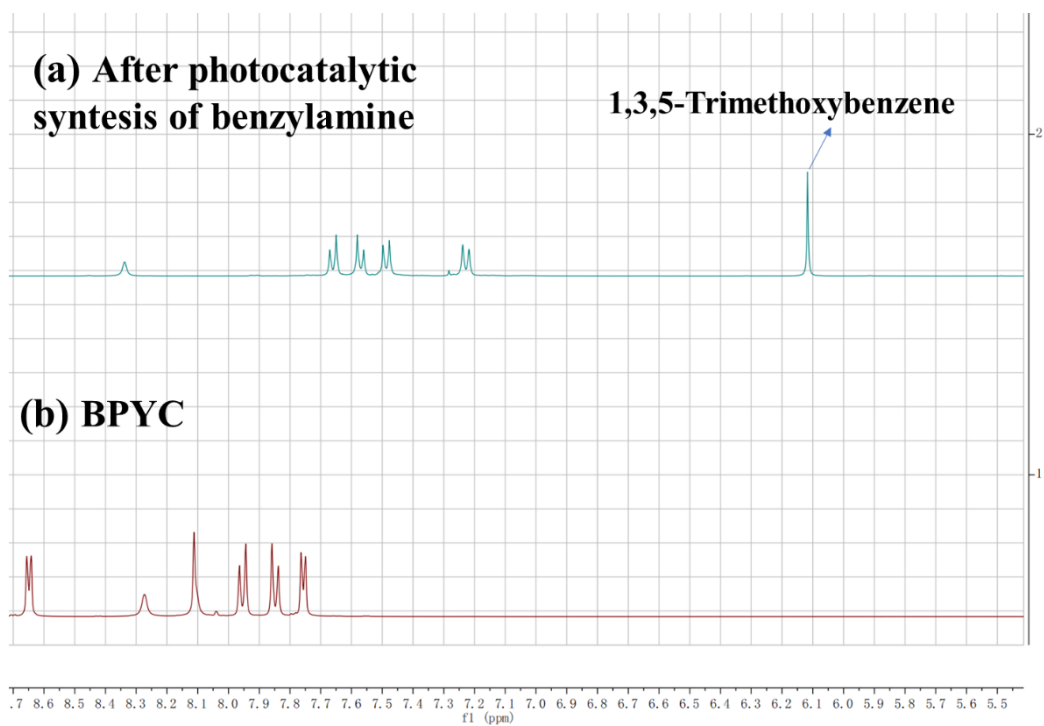


**Figure S9.** <sup>1</sup>H NMR spectra of (a) the reaction solution of photocatalytic oxidation benzylamine using Cu-BPYC as photocatalyst and (b) the BPYC.

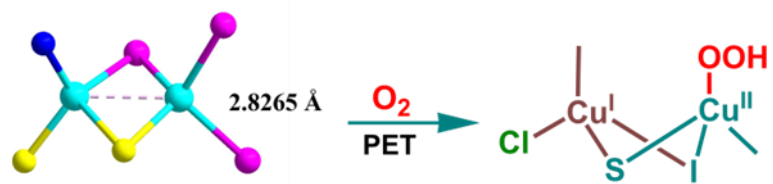


**Figure S10.** Binuclear copper sites in the Cu-BPVC framework for oxygen activation.

## 5. References

- S1 H. L. Huang, X. Jing, J. T. Deng, C. G. Meng, C. Y. Duan, Enzyme-inspired coordination polymers for selective oxidization of C(sp<sup>3</sup>)-H bonds via multiphoton excitation, *J. Am. Chem. Soc.*, 2023, **145**, 2170.
- S2 SMART, Data collection software (version 5.629) (Bruker AXS Inc.; Madison, WI, 2003).
- S3 SAINT, Data reduction software (version 6.45) (Bruker AXS Inc.; Madison, WI, 2003).
- S4 G. M. Sheldrick, SHELXTL97, Program for Crystal Structure Solution (University of Göttingen: Göttingen, Germany, 1997).
- S5. L. Spek, Single-crystal structure validation with the program PLATON. *J. Appl. Cryst.*, 2023, **36**, 7–13.
- S6. C. Yang, S. J. Wan, B. C. Zhu, J. G. Yu and S. W. Cao, *Angew. Chem. Int. Ed.*, 2022, **61**, e202208438.
- S7. J. M. Sun, H. S. Jena, C. Krishnaraj, K. S. Rawat, S. Abednatanzi, J. C. A. Laemont, W. L. Liu, H. Chen, Y. Y. Liu, K. Leus, H. Vrielinck, V. V. Speybroeck and P. V. D. Voort, *Angew. Chem. Int. Ed.*, 2023, **62**, e202216719.
- S8. C. Krishnaraj, H. S. Jena, L. Bourda, A. Laemont, P. Pachfule, J. Roeser, C. V. Chandran, S. Borgmans, S. M. J. Rogge, K. Leus, C. V. Stevens, J. A. Martens, V. V. Speybroeck, E. Breynaert, A. Thomas and P. V. D. Voort, *J. Am. Chem. Soc.*, 2020, **142**, 20107–20116.
- S9. F. Y. Liu, P. Zhou, Y. H. Hou, H. Tan, Y. Liang, J. L. Liang, Q. Zhang, S. J. Guo, M. P. Tong and J. R. Ni, *Nat. Commun.*, 2023, **14**, 4344.
- S10. X. Zhang, P. J. Ma, C. Wang, L. Y. Gan, X. J. Chen, P. Zhang, Y. Wang, H. Li, L. H. Wang, X. Y. Zhou and K. Zheng, *Energy Environ. Sci.*, 2022, **15**, 830–842.
- S11. X. Zhang, H. Su, P. X. Cui, Y. Y. Cao, Z. Y. Teng, Q. T. Zhang, Y. Wang, Y. B. Feng, R. Feng, J. X. Hou, X. Y. Zhou, P. J. Ma, H. W. Hu, K. W. Wang, C. Wang, L. Y. Gan, Y. X. Zhao, Q. H. Liu, T. R. Zhang and K. Zheng, *Nat. Commun.*, 2023, **14**, 7115.
- S12. Y. Luo, B. P. Zhang, C. C. Liu, D. H. Xia, X. W. Ou, Y. P. Cai, Y. Zhou, J. Jiang and B. Han, *Angew. Chem. Int. Ed.*, 2023, **62**, e202305355.

- S13. J. N. Lu, J. J. Liu, L. Z. Dong, J. M. Lin, F. Yu, J. Liu and Y. Q. Lan, *Angew. Chem. Int. Ed.*, 2023, **62**, e202308505.
- S14. Z. F. Li, Z. M. Dong, Z. B. Zhang, B. Q. Wei, C. Meng, W. Zhai, Y. Q. Wang, X. H. Cao, B. Han and Y. H. Liu, *Angew. Chem. Int. Ed.*, 2024, **63**, e202420218.
- S15. Y. X. Liu, L. Li, H. Tan, N. Ye, Y. Gu, S. Q. Zhao, S. P. Zhang, M. C. Luo and S. J. Guo, *J. Am. Chem. Soc.*, 2023, **145**, 19877–19884.
- S16. C. C. Qin, X. D. Wu, L. Tang, X. H. Chen, M. Li, Y. Mou, B. Su, S. B. Wang, C. Y. Feng, J. W. Liu, X. Z. Yuan, Y. L. Zhao and H. Wang, *Nat. Commun.*, 2023, **14**, 5238.
- S17. Q. B. Liao, Q. N. Sun, H. C. Xu, Y. D. Wang, Y. Xu, Z. Y. Li, J. W. Hu, D. Wang, H. J. Li and K. Xi, *Angew. Chem. Int. Ed.*, 2023, **62**, e202310556.
- S18. J. Y. Yue, L. P. Song, Y. F. Fan, Z. X. Pan, P. Yang, Y. Ma, Q. Xu and B. Tang, *Angew. Chem. Int. Ed.*, 2023, **62**, e202309624.
- S19. F. N. Hao, C. Yang, X. M. Lv, F. S. Chen, S. Y. Wang, G. F. Zheng and Q. Han, *Angew. Chem. Int. Ed.*, 2023, **62**, e202315456.
- S20. Y. H. Hou, P. Zhou, F. Y. Liu, Y. Y. Lu, H. Tan, Z. M. Li, M. P. Tong and J. R. Ni, *Angew. Chem. Int. Ed.*, 2024, **63**, e202318562.
- S21. P. J. Li, F. Y. Ge, Y. Yang, T. Y. Wang, X. Y. Zhang, K. Zhang and J. Y. Shen, *Angew. Chem. Int. Ed.*, 2024, **63**, e202319885.
- S22. L. Y. Li, X. M. Lv, Y. Y. Xue, H. B. Shao, G. F. Zheng and Q. Han, *Angew. Chem. Int. Ed.*, 2024, **63**, e202320218.
- S23. H. Yu, F. T. Zhang, Q. Chen, P. K. Zhou, W. D. Xing, S. B. Wang, G. G. Zhang, Y. Jiang, and X. Chen, *Angew. Chem. Int. Ed.*, 2024, **63**, e202402297.
- S24. J. Y. Qiu, K. Meng, Y. Zhang, B. Cheng, J. J. Zhang, L. X. Wang and J. G. Yu, *Adv. Mater.*, 2024, **36**, 2400288.
- S25. J. Y. Yue, J. X. Luo, Z. X. Pan, R. Z. Zhang, P. Yang, Q. Xu and Bo Tang, *Angew. Chem. Int. Ed.*, 2024, **63**, e202405763.
- S26. X. B. Yang, Z. X. Pan, J. Y. Yue, X. W. Li, G. J. Liu, Q. Xu and G. F. Zeng, *Small*, 2024, **20**, 2405907.

- S27. H. H. Sun, Z. B. Zhou, Y. B. Fu, Q. Y. Qi, Z. X. Wang, S. Q. Xu and X. Zhao, *Angew. Chem. Int. Ed.*, 2024, **63**, e202409250.
- S28. M. Q. Zhang, R. C. Liu, F. L. Zhang, H. X. Zhao, X. Li, X. J. Lang and Z. G. Guo, *J. Colloid Interf. Sci.*, 2025, **678**, 1170–1180.
- S29. H. C. Xu, Y. D. Wang, Y. Xu, Q. M. Wang, M. Y. Zhuang, Q. B. Liao and K. Xi, *Angew. Chem. Int. Ed.*, 2024, **63**, e202408802.
- S30. J. Y. Yue, J. X. Luo, Z. X. Pan, Q. Xu, P. Yang and B. Tang, *Angew. Chem. Int. Ed.*, 2024, **63**, e202417115.
- S31. A. Chakraborty, A. Alam, U. Pal, A. Sinha, S. Das, T. S. Dasgupta and P. Pachfule, *Nat. Commun.*, 2025, **16**, 503.
- S32. X. J. Bai, L. L. Guo, T. Q. Jia and Z. F. Hu, *Nat. Commun., J. Mater. Chem. A*, 2024, **12**, 13116–13126.
- S33. C. B. Wu, Z. Y. Teng, C. Yang, F. S. Chen, H. B. Yang, L. Wang, H. X. Xu, B. Liu, G. F. Zheng and Q. Han, *Adv. Mater.*, 2022, **34**, 2110266.
- S34. L. Zhang, C. X. Wang, Q. K. Jiang, P. B. Lyu and Y. X. Xu, *J. Am. Chem. Soc.*, 2024, **146**, 29943–29954.
- S35. H. Zhang, W. X. Wei, K. Chi, Y. Zheng, X. Y. Kong, L. Q. Ye, Y. Zhao and K. A. I. Zhang, *ACS Catal.*, 2024, **14**, 17654–17663.
- S36. J. P. Zhang, H. Lei, Z. J. Li, F. L. Jiang, L. Chen and M. C. Hong, *Angew. Chem. Int. Ed.*, 2024, **63**, e202316998.
- S37. J. Y. Choi, B. Check, X. Y. Fang, S. Blum, H. T. B. Pham, K. Tayman and J. Park, *J. Am. Chem. Soc.*, 2024, **146**, 11319–11327.
- S38. Y. Y. Tang, X. Luo, R. Q. Xia, J. Luo, S. K. Peng, Z. N. Liu, Q. Gao, M. Xie, R. J. Wei, G. H. Ning and D. Li, *Angew. Chem. Int. Ed.*, 2024, **63**, e202408186.
- S39. J. C. Liu, C. Tuo, W. Y. Xiao, M. Y. Qi, Z. T. Wang, H. Li, C. S. Guo, J. L. Song, S. L. Qiu, Y. J. Xu, Q. R. Fang, *Angew. Chem. Int. Ed.*, 2025, **64**, e202416240.